

Photoabsorption near the $L_{II,III}$ Edge of Silicon and Aluminum*

Christian Gähwiller and Frederick C. Brown

Department of Physics and Materials Research Laboratory, University of Illinois, Urbana, Illinois 61801

(Received 6 March 1970)

The absorption coefficients of Al, Si, and SiO were determined in the extreme uv with high spectral resolution, using synchrotron radiation. A detailed comparison of the $L_{II,III}$ edge in the metal and in the semiconductor shows important differences. The spikes observed at the edge in Al are at least consistent with the predictions of recent theory. The silicon L threshold shows the expected spin-orbit splitting of the initial states, but the shape just beyond the edge is not in good agreement with the results of one-electron band theory. The L_I edges are located at 117.4 eV in Al and at 151 eV in Si. Great similarities are noted in the broad structure, 15 or more eV beyond the $L_{II,III}$ edges in the three materials studied and also in Na and Mg films. It is suggested that electron-hole transitions accompanied by collective excitations are involved.

I. INTRODUCTION

The threshold for excitation of the $2p$ electrons or $L_{II,III}$ shell of aluminum occurs near 73 eV in the extreme uv. The corresponding edge for silicon, the next element in the periodic system, occurs at about 100 eV. In the first case, that of a metal, the optical transitions near threshold energy are to unoccupied final states close to the Fermi level, whereas in the second case, an insulator or semiconductor, the transitions are to states near the bottom of the conduction band. In the present paper, we present new high-resolution data on the transmission of thin Al and Si films obtained with the use of synchrotron radiation as a continuum light source. Quantitative values of the absorption coefficients are given so that a detailed comparison can be made between the metal and insulator.

Recent theoretical work¹⁻⁸ shows that the $L_{II,III}$ absorption and emission edges of metals will be modified or enhanced because of the effect of the potential of the core hole on the many electrons near the Fermi surface. Such x-ray singularities or spikes are to be found in the early experimental literature, but recently they have been clearly resolved with the use of synchrotron radiation for the cases of sodium, magnesium, and aluminum.^{9,10} In this paper we present new results on the absorption coefficients of Al and Si at room and at low temperatures. In addition, the optical spectrum of SiO in the range of quantum energies 80–250 eV is reported for the first time.

Although superficially similar, the structure observed near threshold in silicon is less singular than the spikes seen in Al. Moreover, the shape of the silicon edge cannot be adequately explained in terms of density of states from the one-electron band theory. It would appear that besides correct

evaluation of matrix elements, exciton, or other many-body corrections are required. Beyond threshold, the spectra for the two materials Al and Si are remarkably similar and suggestions are given which may help to explain the broad structure above a high-energy edge. The experimental results discussed all involve optical excitation from well-defined initial states to final band states. They illustrate the usefulness of high-resolution spectroscopy in the extreme uv both for revealing many-electron effects in high-energy excitations and for the analysis of band structure in solids.

II. EXPERIMENTAL METHOD AND SAMPLE PREPARATION

The absorption coefficients were obtained by measuring the transmission of thin films of known thicknesses as a function of photon energy using the synchrotron continuum radiated by the 250-MeV electron storage ring at the University of Wisconsin Physical Science Laboratory, Stoughton, Wisc. (Supported in part by the Air Force Office of Scientific Research.) As is well known,¹¹ synchrotron radiation from high-energy electrons covers a spectral range extending from very long wavelengths out to a cutoff in the far uv. This high-energy cutoff shifts to higher energies with increasing electron energy. For the 250-MeV storage ring at Stoughton, useful radiation was found at wavelengths as short as 50 Å. One of the advantages of a storage ring over a synchrotron is that the electrons are truly monoenergetic, and their energy can be varied simply by changing the field in the bending magnets. This allows one to select the most appropriate input spectrum and so to identify and overcome order problems in the spectrometer.

The experimental arrangement is shown in Fig. 1. A narrow cone of synchrotron radiation from

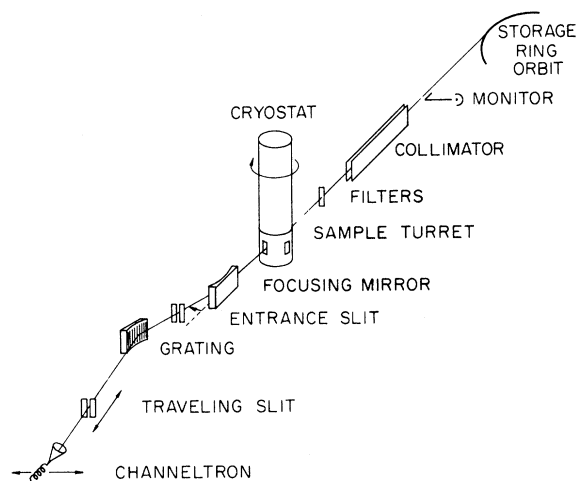


FIG. 1. Outline showing the apparatus used for the measurements. A narrow cone (~ 2 mrad at 100 \AA) of synchrotron radiation is transmitted by the thin film filters and sample and is analyzed by the grazing incidence spectrometer. A common vacuum chamber with ion pumps is not shown.

a small segment of the electron orbit passes through a collimator on a path tangent to the orbit. A common vacuum system used ion and turbomolecular pumps so as to be compatible with the 10^{-10} -Torr vacuum in the storage ring. The purpose of the collimator was not so much to define the beam as to provide a pumping impedance between the ring and the spectrograph where the vacuum was in the range 10^{-7} - 10^{-6} Torr.

The undispersed radiation after passing through selected filters and samples was focused at 4° grazing incidence by means of a gold surfaced mirror onto the $10\text{-}\mu$ entrance slit of the spectrometer. This spectrometer was a 2-m grazing incidence instrument¹² fitted with an exit slit moving along the Rowland circle of a 576 lines per mm grating. Photon counting was employed using a Bendix extended-cone Channeltron as detector moving some distance from, but in phase with, the exit slit. During experimental scans, the signal counting rate was recorded digitally on tape together with the wavelength settings and a signal from the monitor proportional to the beam intensity. The data were processed later by computer in order to yield the absorption coefficients of the samples as a function of photon energy as briefly described in a previous letter.¹³

The wavelength calibration of the spectrometer and the determination of its resolution were obtained by observing the known absorption lines of krypton near 90 eV.¹⁴ For this purpose, a gas

cell with polypropylene windows thinner than 1μ was inserted into the light path in the sample position. The spectral resolution was found to be better than 0.1 \AA in agreement with the calculated value of 0.09 \AA . The results of the calibration were in excellent agreement with a calculated table obtained by a computer analysis of the spectrometer geometry.

The unbacked aluminum films employed in the present investigations were obtained both commercially¹⁵ and by evaporation in the laboratory. In the latter case, thicknesses were determined by the Tolansky method. In the photon energy range covered beyond 70 eV, the reflectivity of the samples was quite small so that the absorption coefficients could be determined reproducibly from the observed transmission and film thickness.

Silicon films were flash evaporated from a tungsten source onto NaCl substrates in a vacuum better than 10^{-6} Torr. It was ascertained that not enough partial pressure of oxygen was present to form appreciable amounts of silicon oxides during the brief periods of evaporation. After floating off onto water, the silicon films were supported on thin Formvar over 80% transparent gold mesh. In each case, the transmission of the supporting substrate was determined prior to measuring the sample. An electron diffraction analysis showed that the evaporated silicon layers were polycrystalline. In addition, the initial part of the silicon $L_{II,III}$ edge was measured for an etched single crystal of silicon, and the results were consistent with those for the evaporated layers. Finally, the silicon monoxide layers were evaporated onto a Formvar substrate from an enclosed source in a standard fashion.

III. RESULTS AND DISCUSSION

A. Aluminum $L_{II,III}$ Absorption

Figure 2 shows the observed absorption coefficient in cm^{-1} for aluminum. The values are in reasonable agreement with previous results,¹⁶⁻¹⁹ and they can be integrated to show that, although only a small fraction of the L -shell absorption is concentrated near the threshold, the total effective number of electrons per atom saturates at about 11 or 12, well before the K edge. It can be seen that sharp spikes are evident at the threshold close to 72.8 eV corresponding to excitation of one of the $L_{II,III}$ core electrons to states near the Fermi surface.

The threshold region is shown on a greatly expanded scale at three different temperatures in Fig. 3. Note that two edges are apparent with positions (300°K) of maximum slope at 72.71 ± 0.01 and 73.15 ± 0.01 eV. The separation of

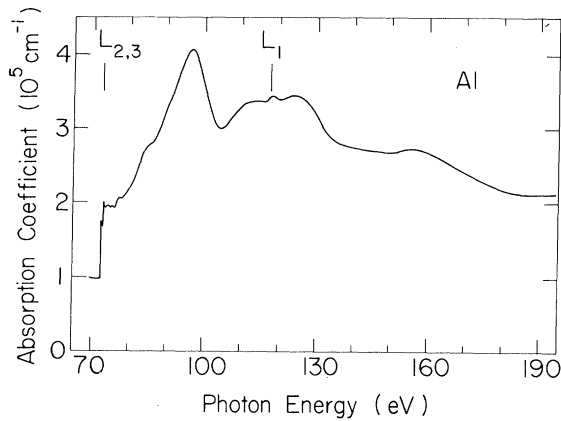


FIG. 2. Absorption coefficient of unbacked aluminum films showing the $L_{II,III}$ edge with spikes near 73 eV and the broad peaks to higher energy. The absolute values of absorption are accurate to within about 20% or better.

these edges corresponds to a spin-orbit splitting of 0.44 ± 0.02 eV. This spin-orbit separation agrees with the absorption results of Codling and Madden¹⁸ and with the emission data of Skinner.²⁰ It cannot be compared with the separation of the $K\alpha_1$ and $K\alpha_2$ lines²¹ unless a correction is applied because of the effect of the K -shell hole on the $L_{II,III}$ splitting. It is interesting to compare the above value of 0.44 eV with the theoretical splitting obtained from a Hartree-Fock calculation. By interpolating between the Herman-Skillman results²² for $Z = 12$ and $Z = 14$, the calculated splitting for aluminum should be close to 0.48 eV.

The width of the threshold rise in Fig. 3 can be understood in terms of a combination of instrument bandwidth (0.04 eV), the effect of temperatures on the Fermi surface, and the width of the initial states due mainly to lifetime effects. From Skinner's emission data, the intrinsic width of the initial states is known to be of the order of 0.02 eV. Note that a slight increase in width of the threshold is discernible upon warming from low temperature. Presumably, this is due to thermal broadening of the Fermi surface. The temperature shift of the threshold is small and difficult to verify.

In contrast with the rising portion of the curves, the singularities or spikes at threshold are little affected by cooling to low temperature. Perhaps the lack of a strong temperature dependence is not surprising, since their widths are of the order of 0.2 eV, which is much greater than kT . As discussed by Hopfield,⁸ the spike phenomena are associated with the creation (by the transient change in core potential) of a very large number of low-energy electron-hole excitations near the

Fermi energy. The dynamical behavior of a core electron excited to a state near the Fermi level is influenced by these many-electron excitations. The x-ray edge problem is analogous to certain infrared divergences involving phonons.

The existing theory¹⁻⁸ of x-ray singularities says that, in the case of a p initial state, the imaginary part of the dielectric response $\epsilon_2 = 2n\kappa = n\alpha c/\omega$ should decrease approximately as $(E - E_0)^{-1/2}$ beyond a threshold E_0 . The asymptotic value at high energy is not given by the theory and so must be taken as an adjustable parameter. Our L edge occurs at 73 eV where $n \approx 1$, and we can neglect the ω^{-1} dependence over the narrow range of energy of Fig. 3. Consequently, it is reasonable to fit the absorption data of Fig. 3 (above background) by superimposing two singularities of the same shape displaced by the known spin-orbit splitting and weighted 2:1 as expected for the $L_{II,III}$ initial state, i. e.,

$$\alpha = \alpha_0 + a/(E - E_1)^{1/2} + \frac{1}{2}\alpha_0 + a/2(E - E_1 + \Delta)^{1/2}. \quad (1)$$

Here E_1 is taken as 72.70 eV, $\Delta = 0.44$ eV, and the two adjustable parameters are found to be

$$\alpha_0 = 0.52 \times 10^5 \text{ cm}^{-1} \quad \text{and} \quad a = 0.1 \times 10^5 \text{ cm}^{-1} (\text{eV})^{1/2}.$$

The fit is quite good over the range of Fig. 3, and the asymptotic value α_0 is reasonable. This result is consistent with, but does not confirm, the approximate $-\frac{1}{2}$ exponent of theory. If we treat the exponents in the denominators of Eq. (1) as adjustable, a log plot indicates that these exponents must lie somewhere in the range $-\frac{1}{2}$ to -1 for reasonable values of α_0 .

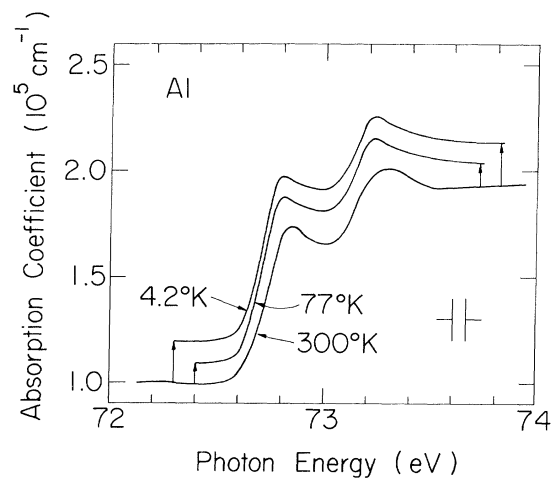


FIG. 3. Showing the $L_{II,III}$ edge of aluminum for three different temperatures approximate on a greatly expanded scale. The two lower-temperature curves have been displaced slightly upwards for purposes of clarity. The instrument bandwidth is 0.04 eV.

The origin of some of the structure on the high-energy side of the $L_{II,III}$ edge is clear. For example, the position of the L_I level in aluminum has been measured by means of electron emission spectroscopy. Early estimates of the L_I position have been found to be grossly in error; however, the revised value of 117.4 eV with respect to the Fermi level has been given by Siegbahn and co-workers.²³ This value is indicated in Fig. 2, and it can be seen that a peak occurs in the absorption spectrum at just such an energy. Slight structure near 76 eV can also be seen in the figure. It is quite possible that this is due to absorption in the thin (approximately 40 Å thick) layers of aluminum oxide which are usually present on the surfaces of specimens such as these.¹⁸ Further remarks about the structure beyond 73 eV are more speculative in nature. The band structure of aluminum has been calculated and is well known.²⁴ On the other hand, the density of states and matrix elements are not known far above the Fermi surface, nor has an optical spectrum been calculated even in the one-electron approximation.^{24a}

It is probably worthwhile to make some general remarks about the broad structure at higher energies. For example, it can be seen that a relatively small amount of the oscillator strength associated with the six $2p$ electrons is concentrated in the vicinity of the spikes at the threshold. The absorption rises to much higher values beyond 90 eV. Sagawa and co-workers²⁵ have suggested that centrifugal barrier effects are important and that the broad rise beyond the edge is due to the increasing importance of $2p$ to nd transitions. Such atomic effects occur especially in elements of higher atomic number.²⁶ An enhancement in absorption cross section beyond the ionization threshold is also characteristic of certain light elements and has been explained in atomic theory by taking many-body effects into account.

It may be useful to point out certain systematics about the high-energy structure and to suggest that plasmon or collective excitations play a role. Broad peaks can be seen beyond the 73-eV edge in Fig. 2 at 97, 112, 125, and 155 eV. Incidentally, at least the first three of these peaks can also be seen in electron energy loss data.^{27,28} A glance at Fig. 4 shows that the general shape of the optical spectrum beyond the $L_{II,III}$ edge is quite similar in silicon. A peak corresponding to the main 97-eV Al resonance also occurs in Si as well as structure higher than the L_I edge. A similar statement can be made about the spectrum above 30 eV in Na and above 50 eV in Mg.¹⁰ We suggest that satellites occur which correspond to a band-to-band transition plus one or more plasmonlike excitations. The situation is somewhat analogous

to longitudinal optical sidebands which frequently occur in lower-energy optical spectra. Whether or not plasmon sidebands are important depends upon how much the electron charge distribution is distorted by the x-ray transition and the predominance of a collective mode. The idea is not entirely new and, in fact, was first discussed by Ferrell²⁹ and later by Nozières and Pines³⁰ as a kind of collective Auger effect. These authors, however, have considered the possibility of an electron-hole excitation together with the production of an ordinary volume plasmon.

Usually the plasmon frequency for a solid is determined experimentally from electron energy loss data or from the optical constants and loss function. In many cases, including the simple metals, a crude estimate of the plasmon frequency ω_p can be obtained from

$$\omega_p^2 = 4\pi e^2 N / m V_0, \quad (2)$$

where N is the number of valence electrons per atom and $V_0 = A/L\rho$ the atomic volume. In Al, for example, $N = 3$, $V_0 = 1.65 \times 10^{-23}$ cm³, so that if the free-electron mass m is used, Eq. (2) yields $\omega_p = 15.8$ eV corresponding to the observed value of 15 eV.

The slight peak superimposed on the rise at 86 eV in Fig. 2 could conceivably be due to a one-plasmon replica of the 73-eV edge and spikes. In the present work on the L edges, we are concerned with a much higher energy range than usual, which brings up the question: Can a collective excitation involving the core as well as valence electrons be excited at energies beyond the $2p$ threshold? Inserting $N = 9$ into Eq. (2) corresponding to six inner plus 3 outer electrons yields an $\hbar\omega_p' = 27.4$ eV as shown under Al in Table I. Evidence for such collective modes together with a core electron excitation might then be found about 27 eV beyond

TABLE I. Plasmon energies $\hbar\omega_p$ calculated from Eq. (2) for N valence electrons per atom and $\hbar\omega_p'$ for $N' = N + 6$ to include the $2p$ core. The experimental values in the last column were taken from periodicities observed beyond the L edge as explained in the text.

	$V_0(10^{-23}$ cm ³)	N	$\hbar\omega_p$ (eV)	Observed $\hbar\omega_p$ (eV)	N'	$\hbar\omega_p'$ (eV)	Observed $\hbar\omega_p'$
Na	4.00	1	5.9	5.8 ^a	7	15.5	17 ^e
Mg	2.32	2	10.9	10.6 ^b	8	21.8	22 ^e
Al	1.65	3	15.8	15.0 ^c	9	27.4	26 ^f
Si	2.00	4	16.6	16.6	10	26.3	25 ^f

^a C. Kunz, Phys. Letters **15**, 312 (1965).

^b C. J. Powell and J. B. Swan, Phys. Rev. **116**, 81 (1959).

^c Reference 27.

^d Reference 31.

^e Reference 10.

^f Present work.

the L edge in Al. Thus, the well-defined peaks in Fig. 2 at 97, 125, and 155 eV could well be associated with the excitation of a $2p$ electron to the Fermi level plus one, two, or three 27-eV collective excitations. Swanson and Powell²⁷ have noted that the 112-eV peak in Al is just 15 eV higher than the main 97-eV peak. It is possible to make very similar assignments for peaks observed¹⁰ beyond the $2p$ edge for Na and for Mg, where the large plasmon energies are simply calculated at 15.5 and 21.8 eV, respectively. See Table I. Detailed theoretical as well as further experimental work is obviously called for.

B. Silicon $L_{II,III}$ Absorption

The absorption spectrum for silicon at and beyond the $L_{II,III}$ threshold is shown in Fig. 4, and the edge is shown on an expanded scale in Fig. 5. These data were obtained from a number of evaporated Si films (thicknesses ranging from 200 to 2500 Å) as well as a thin section etched from a single crystal. Notice that Fig. 4 has the same energy scale and can be directly compared with Fig. 2 for Al, except that the L_{III} edge of Si occurs at 99.6 ± 0.02 eV rather than at 72.7 eV as in Al. Little change was observed in the absorption spectrum for silicon when the samples were cooled from 300 to 77 °K. The threshold did not appear to become appreciably steeper; however, the broad peak at 100.6 eV became slightly more prominent.

The dashed curve in Fig. 4 shows how the effective number of electrons per atom N_{eff} rises above the L threshold. For this purpose, the value of N_{eff} which contributes to the absorption in the range to E_1 was evaluated from the equation:

$$N_{\text{eff}}(E_1) = (2mV_0/e^2\hbar^2) \int_0^{E_1} E \epsilon_2(E) dE, \quad (3)$$

where $E = \hbar\omega$ and the atomic volume $V_0 = A/L\rho$ as before. The reasonable assumption was made that

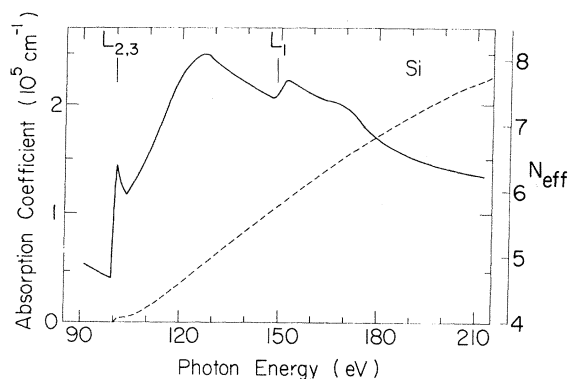


FIG. 4. Absorption coefficient of silicon at and above the L edges.

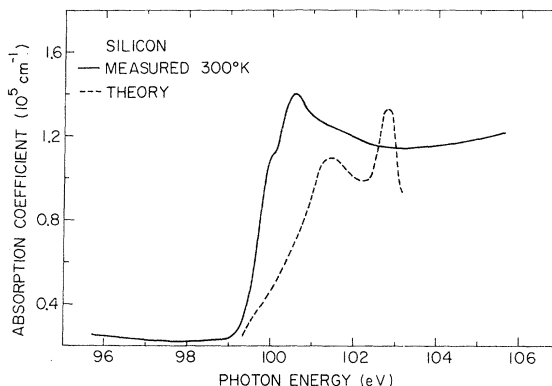


FIG. 5. Showing the measured $L_{II,III}$ absorption edge of silicon on an expanded scale. The dashed line was constructed from the final band density of states as described in the text.

$N_{\text{eff}} = 4$ just before the L_{III} edge.³¹ It can be seen that only a small fraction of the six electrons which make up the $2p$ shell contribute to the absorption in the vicinity of the edge.

The general features of the spectra on the high-energy side of the edge in Si may be explainable as in Al. At least the Si L_I edge can be readily seen in Fig. 4 at 151 eV. This is in good agreement with the interpolated value of 149 eV from electron emission data given in Ref. 23. Perhaps the most important similarities between the spectra for Si and Al are (1) only a small percentage of the $2p$ absorption (N_{eff} less than 0.1 for Si) is concentrated within 5 eV of the threshold, and (2) the absorption rises strongly to broad peaks which begin 15–20 eV beyond the edge. Again, we suggest that this main part of the L absorption is due to an electron-hole excitation plus a kind of collective Auger effect. The volume plasmon frequency for silicon determined from the optical response and energy loss function is 16.6 eV.³¹ Structure with this periodicity is not evident in Fig. 4, except possibly on the low-energy side of the large peak at 125 eV. On the other hand, an estimate of the valence plus core plasmon energy in Si from Eq. (2) gives a value of $\omega'_p = 26.3$ eV. See Table I. Therefore, it may be that the 125-eV peak, absorption just under the L_I region, and a peak near 172 eV correspond to the electron-hole transitions plus one, two, or three such collective excitations.

In analyzing the high-resolution data near the silicon edge (see Fig. 5), it should be noticed that the first component rises to half-height in about 0.4 eV which is a slow rise compared to the aluminum edge. The instrument bandwidth at 100 eV is about 0.07 eV, and from emission data²⁰ the width of the initial states is again about 0.02 eV. Figure 5 also shows that two components separated

by about 0.6 eV are just observable, and these are followed by a decrease which is about one-tenth as fast as in Al. These results are in agreement with earlier data on the silicon edge,^{32,33} but here the high resolution attainable by use of the synchrotron continuum reveals the exact shape of the edge.

Although it is possible to accurately measure the energies of core levels by electron emission spectroscopy, the precise interpretation for insulators and semiconductors is somewhat uncertain. It is thought³⁴ that even in the case of insulators, the binding energy measured by emission (and quoted in the tables³⁵) refers to the Fermi level. Hagström and Karlsson³⁶ have measured the K -shell energy in this manner for evaporated silicon, which may have contained some oxides, but was probably mostly Si. By comparing with L -emission data, they position the L_{III} level at 99.0 and the L_{II} level at 99.6 eV with a percentage error of 0.4. The band gap of silicon is known to be 1.1 eV; therefore, 0.55 eV should be added to the above numbers in order to locate the inner levels with respect to the lowest unoccupied states of the solid. This value of 99.55 eV is remarkably close to the edge position of Fig. 5 and may be fortuitous considering the stated error and uncertainties in locating the Fermi level under the conditions of the electron emission experiment.

It is interesting to compare the observed L spectrum for Si with that expected from the point of view of one-electron band theory. Here the situation is very different from that for aluminum. A pseudopotential calculation has been carried out by Brust^{37,38} and the imaginary part of the dielectric response function evaluated for comparison with the observed near-uv spectrum corresponding to direct transition between valence and conduction bands. A similar comparison has been made by Dresselhaus and Dresselhaus³⁹ using a Fourier transform band theory. In addition, the far-uv spectrum out to about 10 eV has been calculated by Brust and Kane,⁴⁰ including the effects of electron-electron and electron-phonon scattering. Finally, Herman⁴¹ has carried out a self-consistent band calculation in which a small adjustment has been made to fit the experiment.

In principle, the optical spectrum depends upon a summation over initial (filled) and final (empty) bands including an integral over the Brillouin zone as follows³¹:

$$\epsilon_2(\omega) = (4\pi^2 e^2 \hbar / 3m^2 \omega^2) \sum_{n,s} \int_{BZ} [2/(2\pi)^3] \times \delta[\omega_{n,s}(\vec{k}) - \omega] |M_{n,s}(\vec{k})|^2 d^3k, \quad (4)$$

where $\omega_{n,s}(\vec{k}) = [E_s(\vec{k}) - E_n(\vec{k})]/\hbar$

and $|M_{n,s}(\vec{k})|^2 = |(U_{\vec{k},n} | \nabla | U_{\vec{k},s})|^2$,

the square of the dipole matrix elements between periodic parts of the initial and final Bloch functions (direct transitions). Brust found that the matrix elements evaluated between the uppermost valence and the lowest conduction bands were roughly constant over k space. This is not necessarily the case for the $2p$ core to lowest conduction band, nor is it true for the next highest band. It is instructive, however, to consider the matrix elements as constant and equal to some average value as a first approximation. In this case ϵ_2 is given by

$$\epsilon_2(\omega) = (4\pi^2 e^2 / 3m^2 \omega^2) |\overline{M_{ns}}|^2 \sum_{n,s} J_{n,s}(\omega), \quad (5)$$

where $J_{n,s}(\omega)$ is a joint density of states for the bands n and s . Thus $J_{n,s}(\omega)\Delta\omega$ is equal to the number of pairs of states in bands n and s for $E_s(\vec{k}) - E_n(\vec{k})$ lying within a range $\hbar\Delta\omega$ about $\hbar\omega$. The joint density of states together with the $1/\omega^2$ factor in Eq. (5) is, therefore, the important quantity for determining the optical spectrum (assuming constant matrix elements). Singularities or critical points in $J_{n,s}(\omega)$ are thought to determine the important spectral features.

Although the data shown in Fig. 5 give the absorption coefficient $\alpha(\text{cm}^{-1})$, this quantity is closely related to ϵ_2 through the relation $\epsilon_2 = 2n\kappa \approx \alpha\lambda/2\pi$ since the index of refraction n is very close to 1.0 in the high-energy region of the spectrum. Brust and Kane⁴⁰ find that their calculations of ϵ_2 for Ge and Si agree quite well with available reflectivity measurements in the high-energy range out to 10 eV. Their results for Si yield a value of $\epsilon_2 = 1.2$ at $\hbar\omega = 10$ eV. If we extrapolate this to 100 eV using a $1/\omega^2$ dependence, the result is $\epsilon_2 \sim 0.012$. This value of ϵ_2 corresponds to an $\alpha = 6.1 \times 10^4 \text{ cm}^{-1}$, which is only a little larger than the value observed just before the L edge at 99 eV in Fig. 4. On the other hand, a $1/\omega^2$ dependence would follow from constant matrix elements, and it is hard to see why this is the case. For example, another factor of $\omega^{1/2}$ enters if a free-electron density of states applies at very high energy. Undoubtedly, matrix element effects are important and the problem should probably be treated more like the L cross section for atoms.⁴²

Transitions in the edge itself at 99.6 eV are almost certainly from the well-defined p -like initial states to the lowest unoccupied states in the conduction band (Δ_n^p). Refer to Fig. 6. Application of the selection rules for the irreducible representations involved shows that such direct transitions (i. e., Δ_5 to Δ_1 , etc.) are allowed. The same is true for vertical transitions at L_1 and at X_1 but not at Γ_{15} . In any case, the initial density of states are approximately constant, and as a first approximation let us take constant matrix

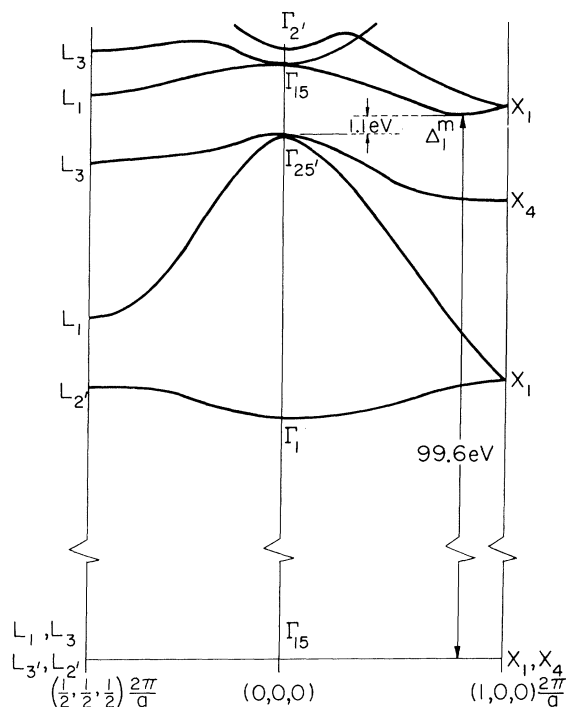


FIG. 6. The lower conduction bands, valence bands, and the $2p$ levels for silicon. Energy is plotted vertically and k vector horizontally in the $[100]$ and $[111]$ directions. Notice the discontinuity in energy scale between the valence bands and core levels. An L_{III} transition to the Δ_1^m conduction-band minimum is indicated.

elements so that Eq. (4) applies and $\epsilon_2(\omega)$ reflects the final density of states.

The dashed curve in Fig. 5 is constructed from Fig. 10 of Ref. 38, which shows the density of states of the lowest two conduction bands calculated from the pseudopotential theory. For this purpose, the threshold (Δ_1^m) was aligned with the observed edge. Two density-of-state curves were superimposed weighted in the ratio 2:1 and shifted by 0.6 eV according to the $L_{II,III}$ spin-orbit splitting.^{22,35} It is seen that rather poor agreement with the edge shape results. The density-of-state curve rises too slowly and forms a double peak much wider than the spin-orbit splitting. In fact, the experimental curve shows two components separated by an amount which is quite close to the calculated spin-orbit value of 0.68 eV.²²

It may be that part of this discrepancy can be removed by a more correct evaluation of the optical spectrum including the matrix elements. There may also be uncertainties in the band calculations along the lines pointed out by Herman.⁴¹ On the other hand, it is hard to see how the particular

spectrum observed can arise from the one-electron theory. The calculated final state densities rise too slowly from threshold, and there will almost certainly be peaks as shown to higher energy. We suggest that important effects due to the core hole are involved, so that the edge is enhanced at the expense of later band-to-band transitions. The formation of an exciton of small binding energy might be the principal effect involved, but the lack of a temperature dependence to the edge is unusual. In this regard, the edge behaves more like the x-ray singularity in aluminum. More theoretical work both on the band and on the x-ray problem is obviously called for.

Finally, in Fig. 7 we show the measured absorption coefficient for an evaporated film of silicon monoxide. A chemical shift for the L edge of several electron volts is seen. Also, this spectrum is superimposed upon a background absorption which is considerably larger than in the case of elemental Si. The SiO spectrum is actually very similar to that reported³³ for SiO₂, except the relative heights of the peaks at 106 and at 109 eV are different. It has been suggested⁴³ that some layers of SiO contain appreciable amounts of Si and of SiO₂. In this regard, the SiO edge rises at 102–103 eV, and no trace of the Si L_{III} edge at 99.6 eV is observable in Fig. 7; therefore, we can say at least that a large percentage of Si was not present in the evaporated SiO layers. This illustrates the potential use of high-resolution spectroscopy in the extreme uv as an analytical tool. Again the silicon L_I transition in the oxide probably contributes to the structure near 155 eV. The general shape of the over-all spectrum beyond the $L_{II,III}$ edge is quite similar to that for both Al and Si, a fact which, as before, suggests the importance of similar atomic or collective effects.

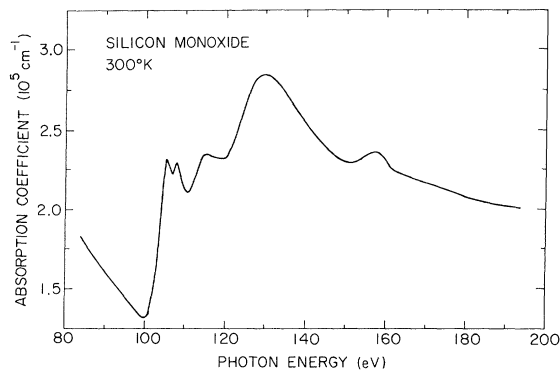


FIG. 7. Absorption coefficient of evaporated films of silicon monoxide.

ACKNOWLEDGMENTS

We are indebted to the staff of the University of Wisconsin Physical Science Laboratory, particularly E. M. Rowe, C. H. Pruett, R. Otte, and F. E. Mills for beam time and assistance at the storage ring. H. Fujita played an important role in the design, assembly, and early operation of the optical apparatus. Electron diffraction studies of the silicon films were expertly carried out by R. Anderson. Helpful discussions were also had

with A. B. Kunz, C. B. Duke, C. T. Sah, P. Handler, and M. A. Elango.

Note added in proof. Recently it has been possible to obtain more data on etched single crystals showing slight but reproducible structure about 3 eV above the edge. Although the spectra are very similar, Fig. 5 should be considered characteristic of evaporated polycrystalline layers [C. Gähwiller and F. C. Brown, Tenth International Conference on the Physics of Semiconductors, Cambridge, Mass., 1970 (unpublished)].

*Work supported in part by the Advanced Research Projects Agency and the U.S. Army Research Office (Durham).

¹G. D. Mahan, Phys. Rev. **163**, 612 (1967).

²B. Roulet, J. Gavoret, and P. Nozières, Phys. Rev. **178**, 1072 (1969).

³P. Nozières, J. Gavoret, and B. Roulet, Phys. Rev. **178**, 1084 (1969).

⁴P. Nozières and C. T. De Dominicis, Phys. Rev. **178**, 1097 (1969).

⁵K. D. Schotte and U. Schotte, Phys. Rev. **182**, 479 (1969).

⁶D. C. Langreth, Phys. Rev. **182**, 973 (1969).

⁷G. A. Ausman and A. Glick, Phys. Rev. **183**, 687 (1969).

⁸J. J. Hopfield, Comments Solid State Phys. **2**, 40 (1969).

⁹R. Haensel, C. Keitel, P. Schreiber, B. Sonntag, and C. Kunz, Phys. Rev. Letters **23**, 528 (1969).

¹⁰C. Kunz, R. Haensel, G. Keitel, P. Schreiber, and B. Sonntag, Symposium on Electronic Density of States, NBS Washington, D. C., 1969 (unpublished).

¹¹J. Schwinger, Phys. Rev. **75**, 1912 (1949); J. D. Jackson, *Classical Electrodynamics* (Wiley, New York, 1963), Chap. 4.

¹²Hilger and Watts, Ltd., see A. H. Gabriel, J. R. Swain, and W. Waller, Rev. Sci. Instr. (London) **42**, 94 (1965).

¹³H. Fujita, C. Gähwiller, and F. C. Brown, Phys. Rev. Letters **22**, 398 (1969).

¹⁴K. Codling and R. P. Madden, Phys. Rev. Letters **12**, 186 (1964); Appl. Opt. **4**, 1433 (1965).

¹⁵Yissum Research Development Co., Hebrew University, Jerusalem, Israel.

¹⁶R. Haensel, C. Kunz, T. Sasaki, and B. Sonntag, J. Appl. Phys. **40**, 3046 (1969).

¹⁷V. A. Fomichev, Fiz. Tverd. Tela **8**, 2892 (1967) [Soviet Phys. Solid State **8**, 2312 (1967)].

¹⁸K. Codling and R. P. Madden, Phys. Rev. **167**, 587 (1968).

¹⁹H. R. Philipp and H. Ehrenreich, J. Appl. Phys. **35**, 1416 (1964).

²⁰H. W. B. Skinner, Phil. Trans. Roy. Soc. London **A239**, 95 (1940).

²¹B. Nordfors, Arkiv Fysik **10**, 20 (1955).

²²F. Herman and S. Skillman, *Atomic Structure Calculations* (Prentice-Hall, Englewood Cliffs, N. J., 1963).

²³A. Fahlman, K. Hamrin, R. Nordberg, C. Nordling,

and K. Siegbahn, Phys. Rev. Letters **14**, 127 (1965).

²⁴V. Heine, Proc. Roy. Soc. (London) **A240**, 340 (1957); **A240**, 354 (1957); **A240**, 361 (1957).

^{24a}The interband contribution to ϵ_2 has recently been calculated out to about 4 eV. See D. Brust, Solid State Commun. **8**, 413 (1970). An atomic calculation of $L_{II,III}$ the high-energy spectrum [J. W. Cooper (private communication)], shows a broad rise extending 50 or more eV beyond the threshold but no other detailed structure.

²⁵T. Sagawa, Y. Iguchi, M. Sasanuma, A. Ejiri, S. Fujiwara, M. Yokota, S. Yamaguchi, M. Nakamura, T. Sasaki, and T. Oshio, J. Phys. Soc. Japan **21**, 2602 (1966).

²⁶U. Fano and J. W. Cooper, Rev. Mod. Phys. **40**, 441 (1968).

²⁷H. Swanson and C. J. Powell, Phys. Rev. **167**, 592 (1968).

²⁸H. Watanabe, J. Appl. Phys. Japan **3**, 804 (1964).

²⁹R. A. Ferrell, Rev. Mod. Phys. **28**, 308 (1956).

³⁰P. Nozières and D. Pines, Phys. Rev. **113**, 1254 (1959).

³¹H. R. Philipp and H. Ehrenreich, Phys. Rev. **129**, 1550 (1963).

³²D. H. Tomboulou and D. E. Bedo, Phys. Rev. **104**, 590 (1956).

³³O. A. Ershov and A. P. Lukirskii, Fiz. Tverd. Tela **8**, 2137 (1966) [Soviet Phys. Solid State **8**, 1699 (1967)].

³⁴S. Hagström, C. Nordling, and K. Siegbahn, in *Alpha-, Beta-, and Gamma-Ray Spectroscopy*, edited by K. Siegbahn (North-Holland, Amsterdam, 1965), Vol. 1, p. 845.

³⁵J. A. Bearden, Rev. Mod. Phys. **39**, 78 (1967).

³⁶S. Hagström and S. E. Karlsson, Arkiv Fysik **26**, 451 (1964).

³⁷David Brust, Phys. Rev. **134**, A1337 (1964).

³⁸David Brust, Phys. Rev. **139**, A489 (1965).

³⁹G. Dresselhaus and M. S. Dresselhaus, Phys. Rev. **160**, 649 (1967).

⁴⁰D. Brust and E. O. Kane, Phys. Rev. **176**, 894 (1968).

⁴¹F. Herman, R. L. Kortum, C. D. Kuglin, and R. A. Short, in *Quantum Theory of Atoms, Molecules and Solids*, edited by Per-Olov Löwdin (Academic, New York, 1966), p. 381.

⁴²H. A. Bethe and E. E. Salpeter, *Quantum Mechanics of One and Two Electron Atoms* (Springer, Berlin, 1957), p. 306.

⁴³M. V. Coleman and D. J. D. Thomas, Phys. Status Solidi **22**, 593 (1967).